Lithium difluorophosphate–modified PEO-based solid-state electrolyte for high-voltage lithium batteries

Jiaxu Tan[1] · Xinhai Li[1,2,3] · Qihou Li[1] · Zhixing Wang[1,2,3] · Huajun Guo[1,2,3] · Guochun Yan[1,2,3] · Jiexi Wang[1,2,3] · Guangchao Li[1]

Abstract

It is of great significance for broadening the electrochemical window of poly(ethylene oxide) (PEO)–based solid electrolyte to match with high voltage lithium cobalt oxide for the commercial application of solid-state lithium-ion batteries. In this paper, $LiPO_2F_2$ was introduced as an additive to increase the stability of PEO-based polymer solid electrolytes. After $LiPO_2F_2$ addition, the oxidative decomposition voltage of PEO increased from 3.8 to 4.8 V. The $LiCoO_2$/PEO-LiTFSI-$LiPO_2F_2$/Li cell showed a specific discharge capacity of 103.2 mAh g^{-1} at 0.2 C after 100 cycles with a capacity retention of 83.8%, which is much better than that of $LiCoO_2$/PEO-LITFSI/Li cell (maintained at 8.7 mAh g^{-1} after only 70 cycles). The improved electrochemical performance can be attributed to the $LiPO_2F_2$ decomposition earlier than PEO during the cycles, and the products acted as a protective layer to stabilize PEO at high voltage. The novel $LiPO_2F_2$-modified PEO electrolyte strategy provides a new approach for solid-state batteries, especially for their high voltage applications.

Keywords $LiPO_2F_2$ · Poly(ethylene oxide) · Solid-state batteries · High voltage

Introduction

Poly(ethylene oxide) (PEO)–based solid-state polymer electrolyte has been identified as one of the most potential candidates for the next generation of solid-state lithium-ion batteries benefiting from its excellent machinability, low cost, and acceptable interfacial stability [1–3]. However, the inherent low oxidatively decomposed voltage (~ 3.9 V vs. Li/Li^+) of PEO restricts its further application to match with commercial $LiCoO_2$ (LCO) and derivatives at high voltage [4, 5]. It is found that LCO can accelerate the PEO degradation

and release gas above 4.2 V (vs. Li^+/Li) [6]. In addition, the dehydrogenation of PEO produces H^+, which is capable to react with lithium bis(trifluoromethane)sulfonimide ($LiN(SO_2CF_3)_2$, LiTFSI) and forms bis(trifluoromethane) sulfonimide ($HN(SO_2CF_3)_2$, HTFSI) in the LCO/PEO-LiTFSI/Li system [7]. As a strong acid, HTFSI is highly corrosive to both LCO and PEO, causing unstable interfaces between PEO and LCO and resulting in the deterioration of battery cycle performance. Therefore, it is very significant to develop effective strategies to improve the high-voltage stability of PEO-based solid-state electrolytes.

Construction of an artificial barrier layer (mainly coating with Li^+-conductive matrix) between LCO and PEO-based electrolyte is one of the efficient strategies to suppress the cathode/electrolyte direct contact and thus decrease the accelerated degradation of PEO induced by Co [8, 9]. As such, the electrochemical window can be increased. For example, Liang et al. applied a thin coating of lithium tantalate (LTO) on high-voltage LCO by atomic layer deposition, making PEO-based solid electrolyte and LCO cathode match well [10]. However, it is hard for a uniform coating to completely inhibit the cathode/electrolyte contact. In addition, the coating layer may increase the interfacial resistance.

✉ Qihou Li
liqihou@csu.edu.cn

✉ Guangchao Li
guangchao_li@csu.edu.cn

1 School of Metallurgy and Environment, Central South University, Changsha 410083, People's Republic of China

2 Engineering Research Center of the Ministry of Education for Advanced Battery Materials, Central South University, Changsha 410083, People's Republic of China

3 Hunan Provincial Key Laboratory of Nonferrous Value-Added Metallurgy, Central South University, Changsha 410083, People's Republic of China

In the liquid electrolytes, some lithium-salt additives, such as lithium bis(oxalato)borate (LiB(C$_2$O$_4$)$_2$, LiBOB) [11], lithium difluoro(oxalate)borate (LiBC$_2$O$_4$F$_2$, LiODFB) [12], and lithium difluorophosphate (LiPO$_2$F$_2$) [13, 14], are able to widen the electrochemical window of the electrolyte via pre-oxidation. In this way, a uniform and stable cathodic electrolyte interface (CEI) layer on the surface of the cathode side can be readily formed [15, 16]. This phenomenon provides ideas for the high-voltage application of such kind additives in the PEO-based solid electrolytes. Recently, Zhao et al. designed a three-salt system of LiBOB, LiNO$_3$, and LiTFSI, which enabled the oxidation potential of PEO up to 4.6 V [17]. However, the reduction and deposition of LiNO$_3$ at the anode side cause the irreversible variation of composition and phase. Therefore, the stability of such a system is still not satisfactory. LiPO$_2$F$_2$ as a successfully applied additive in the liquid electrolyte can form a dense protective film on the cathode surface and shows excellent resistance to temperature [18, 19]. Moreover, LiPO$_2$F$_2$ shows good stability on the anode side. However, as far as we know, the effects of LiPO$_2$F$_2$ on the electrochemical window stability of PEO-based solid-state polymer electrolyte (SPE) are not studied before, let alone applied in high-voltage systems.

Herein, aiming at the incompatibility between PEO and LiCoO$_2$ at high voltage, LiPO$_2$F$_2$ was employed as the high voltage additive to ameliorate PEO-based solid electrolyte. The influences of LiPO$_2$F$_2$ addition on basic electrochemical properties such as ionic conductivity, lithium-ion migration number, electrochemical window, mechanical properties, and thermodynamic properties were comprehensively demonstrated. Moreover, the interface compatibility of PEO-based polymer electrolytes with positive and negative electrodes was revealed as well. When coupled with commercial LCO, the LCO/PEO-LiTFSI-LiPO$_2$F$_2$/Li battery performed stably at 4.2 V and exhibited an initial specific capacity of 123.4 mAh g^{-1} with excellent cycling stability.

Experimental section

Chemicals

The PEO (Sigma, M_w = 4,000,000, 99.9%), LiTFSI (Sigma, 99.95%), and LiPO$_2$F$_2$ (Sigma, 99.9%) were purchased from the commercial appliers and dried at 60 °C in a vacuum oven for 48 h before they were used.

Preparation of PEO-based electrolytes

The LiPO$_2$F$_2$-modified electrolyte was prepared by mixing PEO, LiTFSI, LiPO$_2$F$_2$, and acetonitrile. In detail, 0.2175 g LiTFSI and 0.0050 g LiPO$_2$F$_2$ were dissolved in 15 ml acetonitrile and stirred continuously for 4 h at room temperature

until a homogeneous solution formed. After that, PEO was added into the above solution (EO:Li$^+$ = 15:1 in mole) and finally gel-like slurry with a certain viscosity can be achieved. Then, the slurry was poured into the polytetrafluoroethylene gasket with an inner radius of 17 mm in the glove box (the contents of water and oxygen were below 0.1 ppm). The formed disks were dried at room temperature for 24 h, and further 60 °C for 6 h in the glove box to obtain the polymer solid electrolyte membrane. The basic electrolyte was made in the same way, except without LiPO$_2$F$_2$.

Preparation of solid-state battery

The commercial LCO was employed as electrode active materials and mixed with a binder (poly(vinylidene fluoride), PVDF) and conductive carbon black (Super P) in a weight ratio of 8:1:1. The homogenous slurry can be achieved after the addition of N-methyl pyrrolidone (NMP). And then, it was pasted onto aluminum foil and cut into small pieces with a diameter of 12 mm after drying at 80 °C for 4 h in a vacuum oven. Finally, 2025-type coin cells were assembled with the LCO cathode, PEO solid electrolyte, and Li-metal anode in an argon-filled glovebox.

Electrochemical measurements

Ionic conductivity

The ionic conductivity was measured by alternating current (AC) impedance with the disturbance voltage of 10 mV and scanning frequency range from 1 MHz to 1 Hz to acquire the ontology impedance (R_b) of PEO. The detailed value was calculated by the following equation [20].

$$\sigma = l/(SR_b) \tag{1}$$

where σ is ionic conductivity (S•cm^{-1}), l means the thickness of PEO (cm), R_b stands for the intrinsic impedance of PEO (Ω), and S corresponds to the apparent areal of the electrode (cm^2).

Electrochemical oxidation potential window

The electrochemical oxidation potential window of PEO was determined by linear sweep voltammetry (LSV) tests in Li/PEO/stainless steel (SS) coin-cells. The steel sheet worked as a working electrode (WE), and Li-metal worked as the reference electrode (RE) and counter electrode (CE). The scanning rate was 10 mV s^{-1} in the range of 0–7.0 V and selected the useful data ranged from 2.75 to 6.0 V.

Transference number of lithium-ion (t⁺)

The lithium ion migration number of PEO-based solid electrolyte was measured by constant voltage polarization method and electrochemical impedance spectroscopy (EIS). The polarization curve was obtained under the conditions of a disturbance voltage of 10 mV and a scanning time of 1000 s. The EIS was performed under the conditions of a disturbance voltage of 10 mV and a test frequency of 1 MHz-1 Hz before and after polarization; therefore, the t⁺ value can be calculated according to Eq. (2) [21]

$$t^+ = \frac{I_s(\Delta V - I_0 R_0)}{I_0(\Delta V - I_s R_s)} \qquad (2)$$

where t^+ is the number of lithium ion migration, I_0 and I_s are the initial and steady-state currents, R_0 and R_s represent the initial and steady-state interface impedances, and ΔV means the constant voltage polarization voltage (10 mV).

Stability to lithium and charge–discharge test

The stability of electrolyte to lithium metal was analyzed by testing the lithium symmetric battery. In detail, Li/PEO/Li cell was used to test the polarization voltage at 60 °C at 0.1, 0.2, and 0.3 mA cm⁻² to characterize the stability of the electrolyte/lithium interface. In addition, LCO/PEO/Li coin-cells were assembled and the cycle performance and rate capability were tested in the voltage range of 2.8–4.2 V at 60 °C.

Characterization

The micro-morphology information of the electrolyte was collected by scanning electron microscope (SEM, MIRA3LMH). X-ray diffractometer (XRD, Rigaku TTR-III) was applied to characterize the quantitative analysis of solid electrolytes with the copper targets. The thermal stability of PEO-based solid electrolyte was characterized by thermogravimetric-differential thermal analysis (TG-DSC, TA-Instrument's SDT Q600). The melting transition temperature and crystallinity of PEO-based solid electrolytes were revealed by using differential scanning calorimetry. The crystallinity was calculated by Eq. (3):

$$X_c = \frac{\Delta H_m}{\Delta H_m^0} \times 100\% \qquad (3)$$

where X_c demonstrates the crystallinity of SPE; ΔH_m equals the melting heat of polymer solid electrolyte, corresponding to the melting-related endothermic peak area in the DSC curve; and ΔH_m^0 means the melting heat value of PEO with 100% crystallinity (-213.7 J g⁻¹).

Results and discussion

It can be seen from Fig. 1a that the ionic conductivity reaches the highest when the mass ratio of $LiPO_2F_2$ is 1.0 wt%, implying a certain amount of $LiPO_2F_2$ is beneficial to the improvement of ionic conductivity. The reason might be assigned to that the addition of $LiPO_2F_2$ reduces the crystallinity of the PEO segment, resulting in an improved segment activity and thus making ion transport easier [22, 23]. However, the movement of segments might be limited, and thus the migrations of lithium ions become slow with the increase of $LiPO_2F_2$. In detail, the ionic conductivity of PEO after 1.0 wt% $LiPO_2F_2$ addition is calculated as 1.9×10^{-4} S cm⁻¹ compared to 1.1×10^{-4} S cm⁻¹ without $LiPO_2F_2$. It should be noted that the low conductivity of PEO/lithium polymer electrolyte is attributed to the high crystallinity of PEO which restricts the lithium-ion transfer [24]. The influence of temperature on ionic conductivity of PEO-electrolyte before and after $LiPO_2F_2$ addition is shown in Fig. 1b. The value of ionic conductivity varies from 6.2×10^{-6} S cm⁻¹ at 25 °C to 1.9×10^{-4} S cm⁻¹ at 60 °C, revealing the enhanced conductivities of PEO with the increased temperature. The detailed conductivity value is calculated by Eq. (1) according to EIS spectra (Fig. 1c-d) and shown in Table 1. It is known that the interaction between lithium-ion and PEO chain becomes weakened when the temperature is higher than the melting point of PEO and thus the ionic conductivity can also be improved [25, 26].

The LSV and the galvanostatic step test curves of SS/PEO-LiTFSI-LiPO₂F₂/Li and SS/PEO-LiTFSI/Li are shown in Fig. 2a-b. It can be seen from Fig. 2a that PEO-LiTFSI possesses two decomposition peaks. The one is around 3.2 V, which can be assigned to the decomposition of LiTFSI, and the other one (~ 3.8 V) is affiliated with the decomposition of PEO [27, 28]. As for the PEO-LiTFSI-LiPO₂F₂ system, three decomposition peaks can be found. Peaks around 3.2 and 4.0 V are the decompositions of LiTFSI and LiPO₂F₂, which is similar to PEO-LiTFSI [29, 30]. In addition, the peak around 4.8 V is attributed to the decomposition of PEO. It can be concluded from the above illustrations that the voltage window of PEO widens from 3.8 to 4.8 V after the LiPO₂F₂ addition. This is because LiPO₂F₂ decomposes earlier than PEO and prevents the decomposition of PEO. As illustrated in Fig. 2b, the constant potential steps are performed at 3.8, 4.0, and 4.2 V. The results show that the current of PEO-LiTFSI-LiPO₂F₂ was close to 0 at various voltages, indicating that PEO-LiTFSI-LiPO₂F₂ is more stable than PEO-LiTFSI.

Fig. 1 **a** Ionic conductivity with different contents of $LiPO_2F_2$, **b** ionic conductivity, **c**–**d** impedance spectra of PEO-LiTFSI and PEO-LiTFSI-$LiPO_2F_2$ electrolyte film at different temperatures
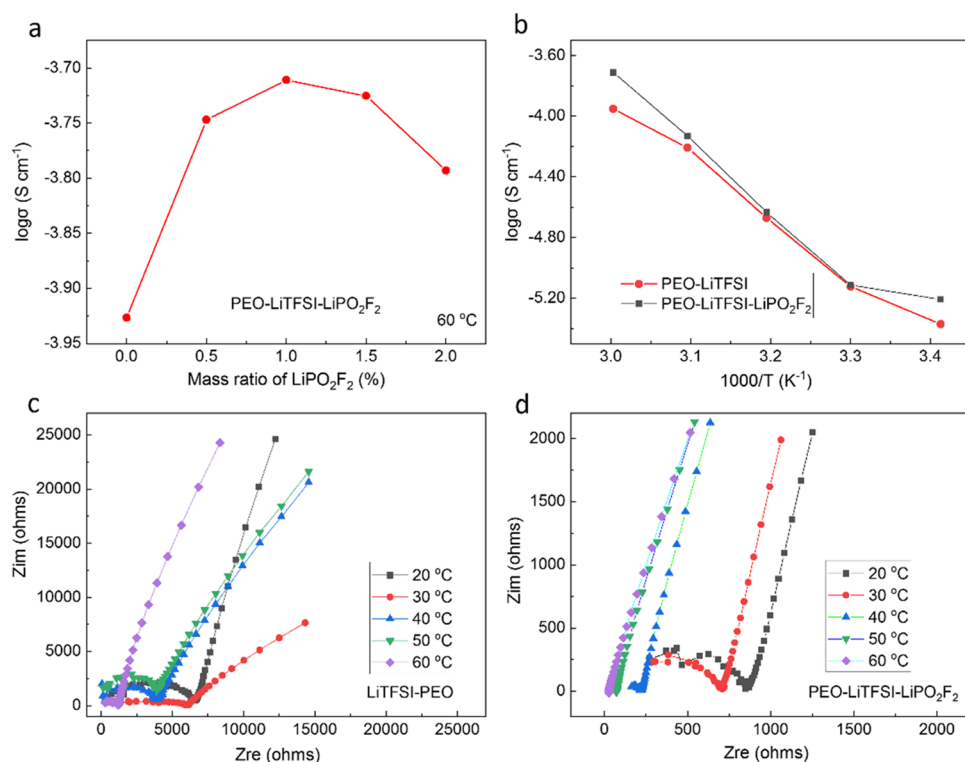

Table 1 Ionic conductivity of polymer solid electrolytes at different temperatures (S cm^{-1})

	20 °C	30 °C	40 °C	50 °C	60 °C
PEO-LiTFSI	4.3×10^{-6}	7.5×10^{-6}	2.1×10^{-5}	6.2×10^{-5}	1.1×10^{-4}
PEO-LiTFSI-$LiPO_2F_2$	6.2×10^{-6}	7.7×10^{-6}	2.3×10^{-5}	7.4×10^{-5}	1.9×10^{-4}

The polymer solid electrolyte is assembled into Li/PEO/Li symmetrical battery, and the polarization voltages of the battery at different current densities are measured. The interface stability between the polymer solid electrolyte and lithium metal anode is characterized by comparing the variation trend of polarization voltage. As shown in Fig. 2c, the polarization voltage fluctuates with the current density. In detail, the polarization voltages of Li/PEO-LiTFSI-$LiPO_2F_2$/Li increase to 32, 61, and 85 mV when the current densities are 0.1, 0.2, and 0.3 mA cm^{-2}. As a contrast, the polarization voltages of Li/PEO-LiTFSI/Li are 33, 66, and 106 mV which is much higher than that of the Li/PEO-LiTFSI-$LiPO_2F_2$/Li system. The higher polarization voltage indicates the higher lithium-ion reaction impedance at the electrode/electrolyte interface [31]. The results manifest that lithium-ion migration ability becomes stronger in Li/PEO-LiTFSI-$LiPO_2F_2$/Li batteries. Moreover, the long-term cycling performance of different electrolyte systems at 0.1 mA cm^{-2} is tested, as shown in Fig. 2d. The Li/PEO-LiTFSI-$LiPO_2F_2$/Li transfers a much smaller polarization value than Li/PEO-LiTFSI/Li (23 mV vs. 34 mV) even after 120 h cycles, revealing the improved cycling performance by the addition of $LiPO_2F_2$.

The smaller electrochemical polarization of LCO/PEO-LiTFSI-$LiPO_2F_2$/Li cells can be attributed to the increased ionic conductivity of the polymer electrolyte after the addition of $LiPO_2F_2$ which results in a more compatible interface interfaces, reduces the electrochemical polarization and concentration polarization. Taking the above illustrations into conclusion, the introduction of $LiPO_2F_2$ enhances the ionic conductivity and reduces polarization which are benefits to the improvement of full-cell performance.

It can be concluded from the thermal stability of PEO in Fig. 3a that PEO keeps stable even when the temperature increases to 800 °C. The melting transition temperature (T_m) and crystallinity (X_c) are characterized by the DSC curve, as shown in Fig. 3b. The results show that the melting transition temperatures of PEO, PEO-LiTFSI, and PEO-LiTFSI-$LiPO_2F_2$ polymer electrolyte membranes are 81.2, 62.2, and 62.7 °C, respectively. It should be noted that the melting transition temperature is related to the ionic conductivity of polymer solid electrolytes [32, 33]. When the temperature is higher than the melting transition temperature, the amorphous areas of PEO increase and the movement of the PEO chain segment enhances, resulting in improved lithium-ion

Fig. 2 Electrochemical parameters tests before and after LiPO$_2$F$_2$ addition. **a** LSV profiles, **b** constant potential step experiments of Li//SS battery with or without LiPO$_2$F$_2$, **c** polarization curves, and **d** cycling performance of Li//Li battery with or without LiPO$_2$F$_2$
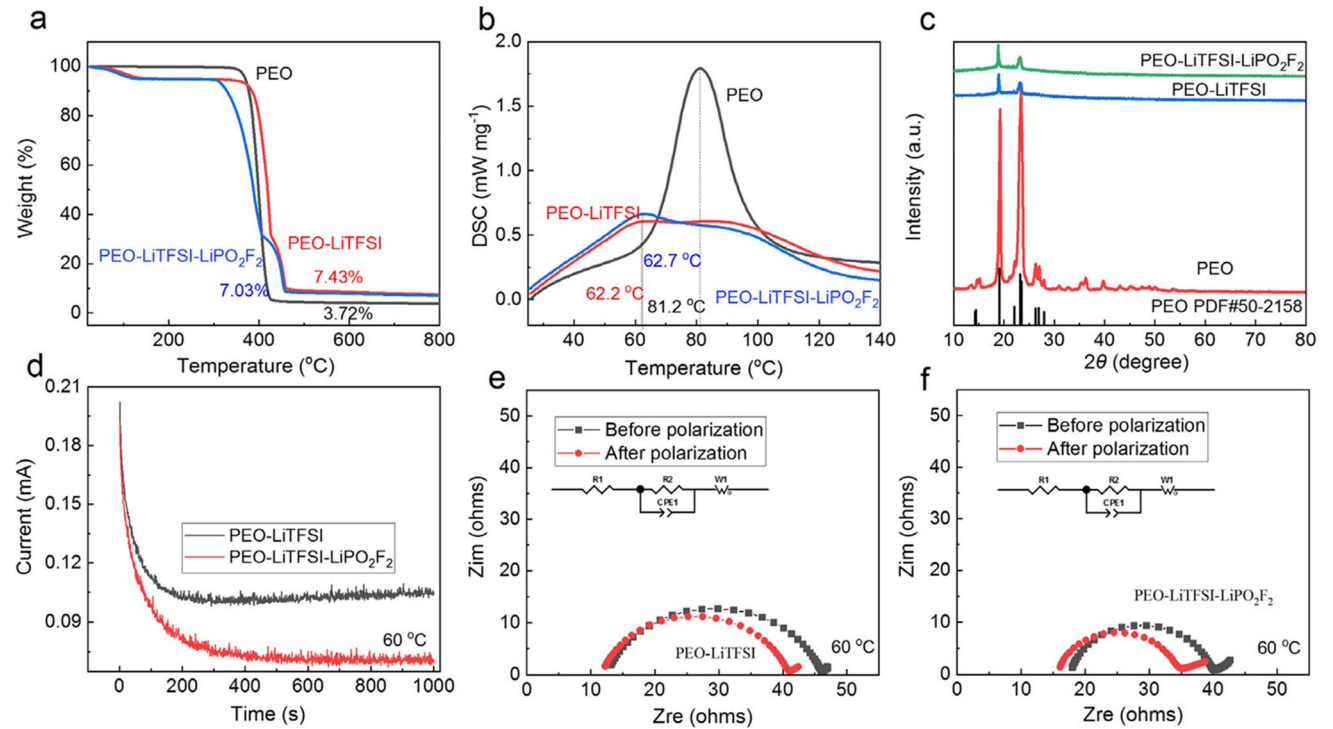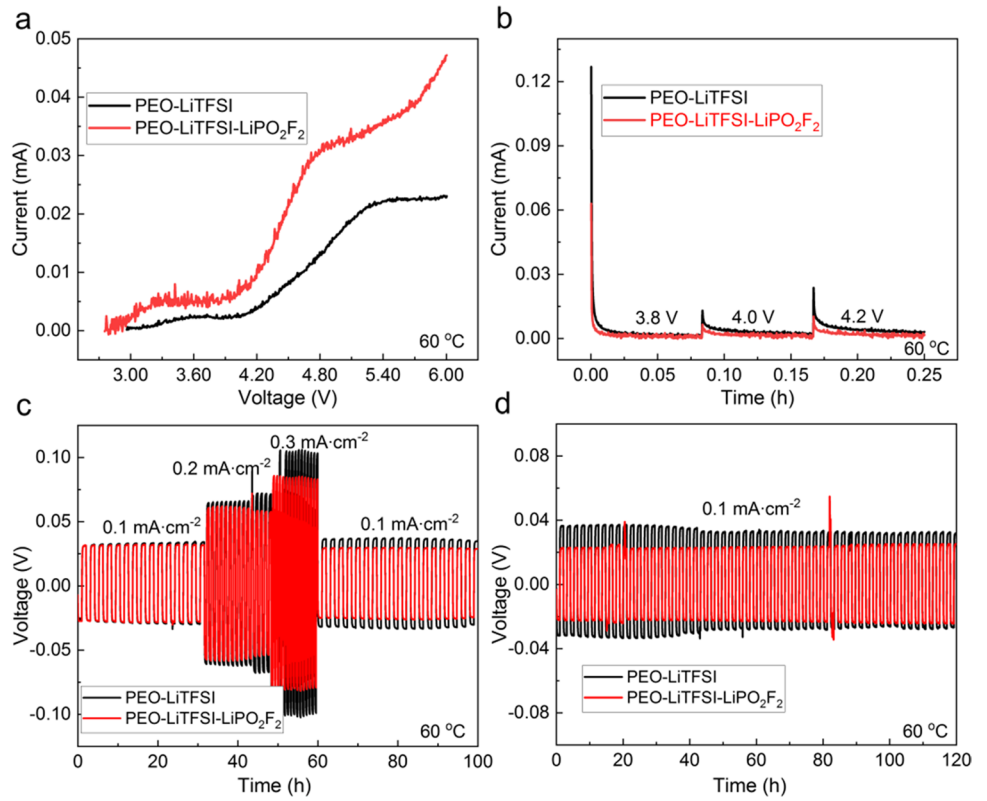

Fig. 3 Thermodynamic and structural properties before and after LiPO$_2$F$_2$ addition. **a–c** TG, DSC, and XRD tests of PEO, PEO-LiTFSI, and PEO-LiTFSI-LiPO$_2$F$_2$ membranes, **d** constant voltage polarization profiles, **e–f** AC impedance spectra at different polarization states of Li//Li battery with or without LiPO$_2$F$_2$

Table 2 Thermodynamic properties of polymer solid electrolyte membranes

Polymer solid electrolyte membrane	Melting transition temperature, T_m (°C)	Heat value, ΔH_m(J·g^{-1})	Crystallinity, X_c (%)
PEO	81.2	180.3	84
PEO-LiTFSI	62.2	73.3	34
PEO-LiTFSI-LiPO$_2$F$_2$	62.7	62.5	29

Table 3 Impedance values before and after cycles of LCO/PEO-LiTFSI/Li and LCO/PEO-LiTFSI-LiPO$_2$F$_2$/Li cells

	LCO/PEO-LiTFSI/Li		LCO/PEO-LiTFSI-LiPO$_2$F$_2$/Li	
	Fresh	After 100 cycles	Fresh	After 100 cycles
R_f(Ω)	16.8	245.2	14.8	9.9
R_s(Ω)	327.5	473.3	99.3	337.4

transport efficiency [34, 35]. Therefore, the low melting transition temperature is beneficial for the improvement of ionic conductivity. The detailed thermodynamic properties are calculated by Eq. (3) and exhibited in Table 2. The above results indicate that the melting transition temperature, endothermic peak area, and crystallinity of polymer solid electrolyte decrease after the addition of LiPO$_2$F$_2$ and lithium salt, which can be further confirmed by XRD results (Fig. 3c). The lithium-ion migration number is a vital parameter to evaluate the lithium-ion conductivity of solid electrolytes. The lithium-ion migration numbers of PEO-LiTFSI and PEO-LiTFSI-LiPO$_2$F$_2$ are calculated according to Eq. (2) and the values are 0.22 and 0.28 by the EIS test results (Fig. 3d-f). The increased lithium-ion migration number makes the formation of Li-ion easier.

Figure 4a-b shows the AC impedance spectra of the LCO/SPE/Li cell before and after cycles. After fitting, the interface impedance (R_s) and volume impedance (R_f) of the LCO/PEO-LiTFSI-LiPO$_2$F$_2$/Li battery before cycling are 14.8 and 99.3 Ω, which both are lower than the LCO/PEO-LiTFSI/Li battery (16.8 and 327.5 Ω). After 100 cycles, the resistance

value increases (Table 3) while the interfacial impedance of LCO/PEO-LiTFSI-LiPO$_2$F$_2$/Li cells is still lower than LCO/PEO-LiTFSI/Li cells. This is consistent with the aforementioned ion conductivity tests and lithium-ion migration number results. The rate performances of LCO/PEO-LiTFSI/Li and LCO/PEO-LiTFSI-LiPO$_2$F$_2$/Li cells are characterized and shown in Fig. 4c. After activated 5 cycles at 0.1 C, the specific discharge capacity of the battery increased. However, the capacity of LCO/PEO-LiTFSI/Li is almost zero when the current density increased to 2–3 C. When the current density returns to 0.1 C, the capacity increases after multiple activations. The cycling performance of LCO/SPE/Li battery with different electrolyte systems is tested and shown in Fig. 4d. After 100 cycles, the specific capacity of LCO/PEO-LiTFSI-LiPO$_2$F$_2$/Li battery decays from 123.4 mAh g^{-1} to 103.2 mAh g^{-1} while the discharge specific capacity of LCO/PEO-LiTFSI/Li decreases from 76.5 mAh g^{-1} to 4.8 mAh g^{-1}, which reveals a serious capacity attenuation after cycles.

The dQ/dV curves of the LCO/PEO/Li battery before and after cycling are shown in Fig. 4e-f. At the beginning
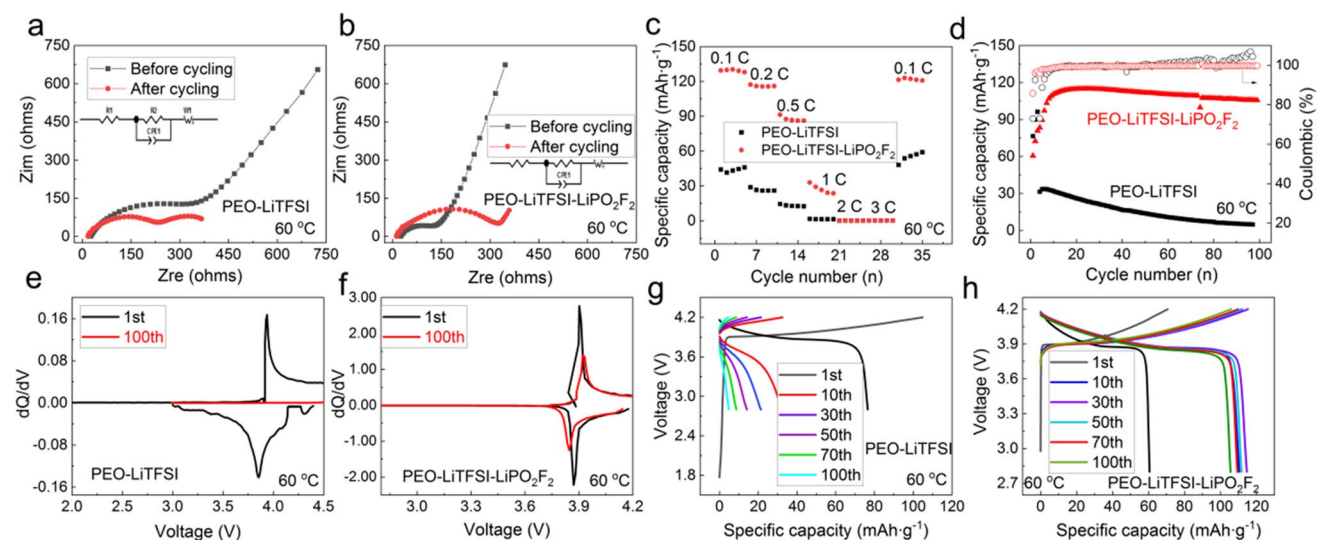
Fig. 4 Electrochemical performance of LCO//Li battery with or without LiPO$_2$F$_2$ as solid-state electrolyte. **a–b** AC impedance spectra before and after cycles, **c** rates capability, **d** cycling stability test at 0.2 C, **e–f** dQ/dV curves, **g–h** charge–discharge profiles (voltage range: 2.8–4.2 V, 1 C = 145 mA g^{-1})

of the cycle, LCO/PEO-LiTFSI-LiPO$_2$F$_2$/Li cells possess lower potential difference (0.03 V) than LCO/PEO-LiTFSI/Li cells (0.08 V). After 100 cycles, the dQ/dV peak of the redox reaction cannot be found in the LCO/PEO-LiTFSI/Li cells, indicating LCO/PEO-LiTFSI-LiPO$_2$F$_2$/Li cells transfer higher reversibility. In other words, the interface of the LCO/PEO-LiTFSI/Li battery is unstable and the addition of LiPO$_2$F$_2$ inhibits the side reaction between the electrode and electrolyte interface during cycles. As shown in Fig. 4g-h, the discharge specific capacity of LCO/PEO-LiTFSI-LiPO$_2$F$_2$/Li battery at 1, 10, 30, 50, 70, and 100 cycles are 123.4, 110.5, 114.7, 111.5, 109.4, and 103.4 mAh g^{-1}, which are also better than LCO/PEO-LiTFSI/Li (76.5, 31.9, 21.4, 14.2, 8.7, 4.8 mAh g^{-1}). It can make a conclusion that the cycle stability of PEO-based electrolytes can be effectively improved when matched with high-voltage LCO by the addition of the LiPO$_2$F$_2$ additive.

SEM is applied to characterize the morphology transformation of LCO/PEO-LiTFSI/Li and LCO/PEO-LiTFSI-LiPO$_2$F$_2$/Li cells after 100 cycles, as shown in Fig. 5a and d. After 100 cycles, a layer of membrane covers on the surface can be only found in LCO/PEO-LiTFSI-LiPO$_2$F$_2$/Li. It is speculated that the film is derived from the LiPO$_2$F$_2$ decomposition during cycles. To verify the conjecture, the cells after cycles are disassembled and the LCO/PEO-LiTFSI/Li and LCO/PEO-LiTFSI-LiPO$_2$F$_2$/Li three-layer structure are scanned by EPMA to test the element distribution. In

specifically, the Co element exists in the anode (Fig. 5b and e). When it comes to P element distribution, it can be only detected in LCO/PEO-LiTFSI-LiPO$_2$F$_2$/Li cells (Fig. 5c and f), which certifies the previous conjecture holds. Taking the above results into account, the LiPO$_2$F$_2$ decomposes before PEO during cycles and protects it from failure. In this way, the stability of PEO is improved and thus can match with LCO at high voltage.

Conclusions

In this work, LiPO$_2$F$_2$ was successfully applied as a high-voltage additive to enlarge the narrow electrochemical window of PEO-based solid electrolytes. On one side, the addition of LiPO$_2$F$_2$ can improve the ion conductivity by decreasing the crystallinity of PEO, and helped to enhance the Li$^+$ transportation. More importantly, the LiPO$_2$F$_2$ decomposed before PEO during cycles and formed a dense and stable CEI on the cathode surface which can protect PEO from decomposition under high voltage. As a result, the electrochemical performance of PEO at high voltage was largely improved with 1.0 wt% LiPO$_2$F$_2$ addition. When assembled with commercial LCO and Li metal into a solid-state battery, a high specific capacity of 123.4 mAh g^{-1} and excellent cycling stability of 83.8% after 100 cycles were achieved. This work provides an effective method to improve
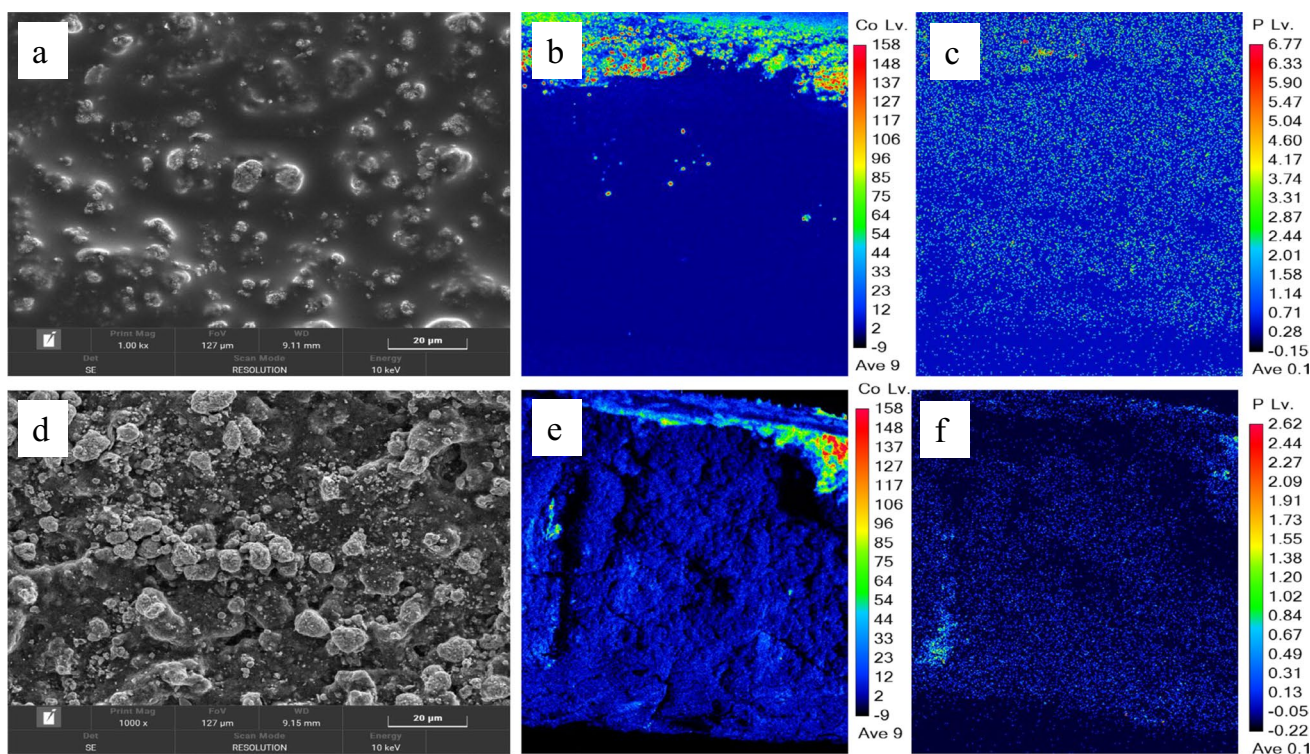

Fig. 5 SEM images and element analysis of LCO/PEO-LiTFSI-LiPO$_2$F$_2$/Li cell (**a–c**) and LCO/PEO-LiTFSI/Li cell (**d–f**) after 100 cycles

the stability of PEO solid electrolytes at high voltage and thus it can match with the commercial cathode. In this way, the practical application of solid-state batteries was largely put forward.

Declarations

Conflict of interest The authors declare no competing interests.

References

1. Sahore R, Yang G, Chen X et al (2022) A bilayer electrolyte design to enable high-areal-capacity composite cathodes in polymer electrolytes based solid-state lithium metal batteries. ACS Appl Energy Mater 5(2):1409–1413
2. Yi M, Li J, Fan X et al (2021) Single crystal Ni-rich layered cathodes enabling superior performance in all-solid-state batteries with PEO-based solid electrolytes. J Mater Chem A 9(31):16787–16797
3. Guo Z, Wu Y, Li X et al (2022) Lowering the operating temperature of PEO-based solid-state lithium batteries via inorganic hybridization. Ionics 28(2):779–788
4. Yan T, Zhu L, Wu Y et al (2021) Enlarging potential window and enhancing stability of poly(ethylene oxide)-based composite solid electrolyte via succinonitrile additive for advanced solid lithium batteries. Funct Mater Lett 14(3):2141004
5. Butzelaar AJ, Rring P, Mach TP et al (2021) Styrene-based poly(ethylene oxide) side-chain block copolymers as solid polymer electrolytes for high-voltage lithium-metal batteries. ACS Appl Mater Interfaces 13(33):39257–39270
6. Pan K, Zhang L, Qian W et al (2020) A flexible ceramic/polymer hybrid solid electrolyte for solid-state lithium metal batteries. Adv Mater 32(17):2000399
7. Nie K, Wang X, Qiu J et al (2020) Increasing poly(ethylene oxide) stability to 4.5 V by surface coating of the cathode. ACS Energy Letters 5(3):826–832
8. Cai D, Wu X, Xiang J et al (2021) Ionic-liquid-containing polymer interlayer modified PEO-based electrolyte for stable high-voltage solid-state lithium metal battery. Chem Eng J 424:130522
9. Liang J, Hwang S, Li S et al (2020) Stabilizing and understanding the interface between nickel-rich cathode and PEO-based electrolyte by lithium niobium oxide coating for high-performance all-solid-state batteries. Nano Energy 78:105107
10. Liang J, Sun Y, Zhao Y et al (2020) Engineering the conductive carbon/PEO interface to stabilize solid polymer electrolytes for all-solid-state high voltage LiCoO$_2$ batteries. J Mater Chem A 8:2769–2776
11. Sheina L, Ivanov A, Karaseva E et al (2022) The effect of lithium bis(oxalato)borate on the galvanostatic charge-discharge cycling of lithium electrode in sulfolane solutions of lithium perchlorate. Russ J Electrochem 58(3):210–215
12. Zhou H, Xiao K, Li J et al (2016) Lithium difluoro(oxalate)borate and LiBF$_4$ blend salts electrolyte for LiNi$_{0.5}$Mn$_{1.5}$O$_4$ cathode material. J Power Sources 302:274–282
13. Li L, Deng Y, Duan H et al (2022) LiF and LiNO$_3$ as synergistic additives for PEO-PVDF/LLZTO-based composite electrolyte towards high-voltage lithium batteries with dual-interfaces stability. J Energy Chem 65:319–328
14. Jiang B, Li J, Luo B et al (2021) LiPO$_2$F$_2$ electrolyte additive for high-performance Li-rich cathode material. J Energy Chem 60:564–571
15. Zhao W, Zheng G, Lin M et al (2018) Toward a stable solid-electrolyte-interfaces on nickel-rich cathodes: LiPO$_2$F$_2$ salt-type additive and its working mechanism for LiNi$_{0.5}$Mn$_{0.25}$Co$_{0.25}$O$_2$ cathodes. J Power Sources 380:149–157
16. Kim K, Jang J, Park I et al (2015) A combination of lithium difluorophosphate and vinylene carbonate as reducible additives to improve cycling performance of graphite electrodes at high rates. Electrochem Commun 61:121–124
17. Zhao Q, Chen P, Li S et al (2019) Solid-state polymer electrolytes stabilized by task-specific salt additives. J Mater Chem A 7(13):7823–7830
18. Ding W, Lv F, Xu N et al (2021) Polyethylene oxide-based solid-state composite polymer electrolytes for rechargeable lithium batteries. ACS Appl Energy Mater 4(5):4581–4601
19. Sun C, Yusuf A, Li S et al (2021) Metal organic frameworks enabled rational design of multifunctional PEO-based solid polymer electrolytes. Chem Eng J 414:128702
20. Verma ML, Sahu HD et al (2015) Ionic conductivity and dielectric behavior of PEO-based silver ion conducting nanocomposite polymer electrolytes. Ionics 21(12):3223–3231
21. Evans J, Vincent C, Bruce P et al (1987) Electrochemical measurement of transference numbers in polymer electrolytes[J]. Polymer 28(13):2324–2328
22. Gabriele L, Patric G, Petr S et al (1987) Unique carbonate-based single ion conducting block copolymers enabling high-voltage, all-solid-state lithium metal batteries. Macromolecules 54(14):6911–6924
23. Zhai H, Xu P, Ning M et al (2017) A flexible solid composite electrolyte with vertically aligned and connected ion-conducting nanoparticles for lithium batteries. Nano Lett 17(5):3182–3187
24. Wang H, Cui X, Zhang C et al (2020) Promotion of ionic conductivity of PEO-based solid electrolyte using ultrasonic vibration. Polymers 12(9):1889
25. Plocharsk J, Wieczorek W (1988) PEO based composite solid electrolyte containing NASICON. Solid State Ionics 28(2):979–982
26. Li C, Xue P, Chen L et al (2022) Reducing the crystallinity of PEO-based composite electrolyte for high performance lithium batteries. Compos Part B: Eng 234:109729
27. Qiu J, Liu X, Chen R et al (2020) Enabling stable cycling of 4.2 V high-voltage all-solid-state batteries with PEO-based solid electrolyte. Adv Funct Mater 30(22):1909392
28. Homann G, Stolz L, Nair J et al (2020) Poly(ethylene oxide) based electrolyte for solid-state-lithium-batteries with high voltage positive electrodes: evaluating the role of electrolyte oxidation in rapid cell failure. Sci Rep 10(1):4930
29. Song W (2019) LiPO$_2$F$_2$ as a LiPF$_6$ stablizer additive to improve the high-temperature performance of the NCM811/SiO$_x$@C battery. Int J Electrochem Sci 14:9069–9079
30. Mabuchi T, Nakajima K, Tokumasu T et al (2021) Molecular dynamics study of ion transport in polymer electrolytes of all-solid-state Li-ion batteries. Micromachines 12(9):1012
31. Han X, Wu T, Gu L et al (2020) A Li-based MOF-derived multifunctional PEO polymer solid-state electrolyte for lithium energy storage. New J Chem 46(8):3747–3753

32. Xu H, Chien P, Shi J et al (2019) High-performance all-solid-state batteries enabled by salt bonding to perovskite in poly(ethylene oxide). Proc Natl Acad Sci 116(38):18815–18821

33. Kim D, Park J, Gong M et al (1994) Effect of grafting degree and side PEO chain length on the ionic conductivities of NBR-g-PEO based polymer electrolytes. Polym Eng Sci 34(17):1305–1313

34. Peng B, Yao Y, Chen Q et al (2015) Solid-state high-resolution NMR studies on PEO-based crystalline solid polymer electrolytes for lithium-ion battery. Annu Rep NMR Spectrosc 85:1–26

35. Brooks D, Merinov B, Goddard W et al (2018) Atomistic description of ionic diffusion in PEO-LiTFSI: effect of temperature, molecular weight, and ionic concentration. Macromolecules 51(21):8987–8995